



**ARTICLE**

# Experimental Study on the Axial Compression Behavior of Short Columns of Steel-Fiber-Reinforced Recycled Aggregate Concrete

Chunyang Liu<sup>1,2,\*</sup>, Jia Xu<sup>1</sup>, Yifan Gu<sup>1</sup> and Ruofan Shi<sup>1</sup>

<sup>1</sup>Department of Civil Engineering, Shandong Jianzhu University, Jinan, China

<sup>2</sup>Key Laboratory of Building Structural Retrofitting and Underground Space Engineering, Shandong Jianzhu University, Jinan, China

\*Corresponding Author: Chunyang Liu. Email: liucy2011@sdjzu.edu.cn

Received: 30 March 2021 Accepted: 25 May 2021

## ABSTRACT

In order to study the axial compression performances of short columns made of recycled aggregate concrete, four samples were designed with different recycled aggregate replacement rates and carbon fibre reinforced plastics (CFRP) sheets. Then, monotonic loading was implemented to assess the variation trends of their axial compression properties. The ABAQUS finite element software was also used to determine the compression performances. Good agreement between experimental and numerical results has been found for the different parameters being considered. As shown by the results, recycled coarse aggregates result in improved ductility and better deformation performance of the specimens. The failure of specimens caused by pre damage can be compensated by using CFRP sheets, by which both the resistance to deformation and the axial carrying capacity of columns can be increased.

## KEYWORDS

Recycled aggregate concrete; short column; axial pressure performance; ABAQUS finite element analysis; carrying capacity calculation

## 1 Introduction

With the acceleration of urbanization, old buildings are increasingly being demolished, and construction waste can be seen everywhere. However, the traditional disposal methods of construction waste are no longer compatible with the concept of green and sustainable development in modern society. Recently, a new treatment method of using construction waste to make recycled aggregate concrete has been proposed. Recycled aggregate concrete refers to concrete made by crushing construction solid waste to replace natural coarse aggregates or fine aggregates. At present, recycled aggregate concrete is sparingly used in structures, and its technical research and application has become a topic of common concern for researchers at home and abroad [1].

Compared with natural aggregates, recycled aggregates have higher water absorption. This effect can be compensated by calculating the water consumption of the recycled aggregate or pre-absorbing the recycled aggregate while designing the composition. Thomas et al. [2] and Kou et al. [3] analysed the durability properties of concrete incorporating recycled aggregate. The results show, the durability of the concretes



made with recycled aggregate is worse due to the intrinsic porosity of them. Dimitriou et al. [4] presented the effect of recycled aggregate to concrete and a treatment method utilized to improve the properties of recycled aggregate, by reducing the amount of the adhered mortar, and the mechanical properties and durability of recycled aggregate concrete were improved using the proposed methodologies. Carneiro et al. [5] investigated the influence of steel fiber reinforcement on the stress–strain behavior of concrete made with recycled aggregates. The research results show that the addition of steel fiber and recycled aggregate increased the mechanical strength and modified the fracture process relative to that of the reference concrete. Ramesh et al. [6] implemented regression models based on the recycled aggregate and steel fiber contents in the steel fiber reinforced recycled aggregate concrete mixes to predict their split-tensile strength, compressive strength and elastic modulus.

At present, the research on recycled aggregate concrete materials has been relatively sufficient. Some researchers have further conducted a large number of experimental studies on recycled aggregate concrete columns. Xiao et al. [7,8] studied recycled aggregate concrete made of recycled aggregates with a particle size range of 5 mm–31.5 mm, and studied the effects of recycled aggregate replacement rate and eccentricity on recycled aggregate concrete columns. Their results showed that the crack development stage of the specimen with eccentricity is longer. For the specimen with small eccentricity, the crack resistance of recycled aggregate concrete column is stronger than that of natural concrete. However, for the specimen with large eccentricity, the crack development speed is faster, which affects the replacement rate of recycled aggregate. Liu et al. [9] designed four different beams and studied the performances of high-strength concrete beams including steel fibers and large-particle recycled aggregates. The results show that the shear failure mode of recycled concrete beams is similar to that of ordinary concrete beams. The shear carrying capacity of high-strength concrete beams including steel fibers and large-particle recycled coarse aggregates grows with an increase in the replacement rate of recycled coarse aggregates. Reinforcement with CFRP sheets can significantly improve the beam's shear carrying capacity and overall resistance to deformation. Cao et al. [10–12] studied the influence of column section type on the compression performance of recycled aggregate concrete columns. The particle size range of recycled aggregate is 5 mm–25 mm. They found that the ductility of recycled aggregate concrete columns is slightly better than that of natural concrete columns, and the energy dissipation capacity of circular section columns is better than that of square section columns. Choi et al. [13] studied investigates the compressive behavior of reinforced concrete columns that are made from recycled aggregate and are subjected to monotonic uniaxial loading. The test results and the calculated strengths for the axial load capacity of the recycled aggregate concrete columns using the above approach indicates that recycled aggregate concrete columns fulfill the ACI design strength criteria. Xu et al. [14] presented a review of experimental tests performed for the characterization of the mechanical behavior of FRP-concrete members realized employing recycled aggregate concrete. Xiong et al. [15] introduced the compressive behavior of FRP-confined steel-reinforced concrete columns using recycled aggregate concrete. It has been revealed that the FRP-confined steel-reinforced concrete columns with recycled aggregate concrete had similar compressive behavior as the FRP-confined steel-reinforced concrete columns with normal aggregate concrete although the use of recycled aggregate concrete slightly decreased the load-carrying capacity. Sushree et al. [16] studied the influence of different fly ash contents instead of cement on the axial compression performance of reinforced concrete columns when 100% recycled coarse aggregate was replaced. The results show that the peak load of recycled aggregate concrete columns mixed with fly ash is slightly higher than that of ordinary concrete columns. Wu et al. [17,18] studied recycled mixed concrete made from large-size waste concrete blocks with a characteristic size of 50 mm–400 mm, and conducted axial compression performance tests on the recycled mixed concrete short columns. They found that the compressive carrying capacity of the block reinforced mixed short column needs to be multiplied by 0.9 on the basis of the current standard calculation. Jia [19] and Huang [20] studied the

axial compression performance of CFRP strip-constrained steel recycled concrete columns and CFRP-constrained steel recycled concrete columns. The results show that: The failure mode of the CFRP strip-constrained recycled concrete column under axial load is roughly the same, showing brittle failure, and the calculated value of the axial compression carrying capacity is in good agreement with the experimental value. The CFRP-constrained steel recycled concrete column has good axial compression performance, and the axial compression carrying capacity of the specimen is effectively improved. The built-in section steel can improve the ductility of the specimen.

The existing research mainly focuses on recycled aggregates in the particle size range of 5 mm–31.5 mm. There is a lack of research on the use of recycled aggregates in the particle size range of 31.5 mm–50 mm. In this paper, the concrete made of recycled aggregates with a particle size range of 31.5 mm–50 mm is called large particle size recycled aggregate concrete. The study of large particle size recycled aggregate concrete is conducive to saving costs, reducing energy consumption, and reducing the damage caused by the aggregate processing. In this experiment, a total of four large-diameter recycled aggregate concrete short columns were fabricated. One of the specimens with 100% replacement rate of recycled coarse aggregate was pre-damaged and reinforced with CFRP cloth. The axial compression performance was studied, the carrying capacity, strength and failure form of the specimens were analyzed, and the ABAQUS finite element software was used to perform numerical simulation analysis on the specimens. Based on the specification, a calculation formula for the axial compression carrying capacity of large-particle recycled aggregate concrete columns was proposed, in order to provide a basis for the application of large-particle recycled aggregate concrete in practical engineering.

## 2 Test Survey

### 2.1 Raw Material

The recycled coarse aggregate used in this experiment was made by crushing the aggregate generated from the dismantling of waste residential buildings. The cement is P.O42.5 grade natural Portland cement, and it meets the relevant regulations of “General Portland Cement” GB 175-2007. The particle size of natural aggregate is 5–20 mm. The particle size range of recycled coarse aggregate is 31.5 mm–50 mm and the fine aggregate is natural river sand. The steel fiber is copper-plated high-strength steel fiber, and the diameter of the steel fiber is 0.2 mm–0.25 mm, the length is 12–14 mm, and the aspect ratio is 48-70, and tensile strength greater than 2850 Mpa. The admixture is Grade I fly ash and fumed silica. The density of fly ash is 2.6 kg/m<sup>3</sup>, and specific surface area of fumed silica is 19 m<sup>2</sup>/g. The superplasticizer is a liquid polycarboxylic acid water reducer, and water reduction rate is not less than 30%.

### 2.2 Specimen Design

Three groups of 150 mm × 150 mm × 150 mm cube test blocks were reserved for the test and the specimens were maintained at the same time. The concrete mix ratio is shown in [Tab. 1](#). The compressive strength of recycled aggregate concrete was measured. The test results are shown in [Tab. 2](#). The longitudinal steel bars were sampled and stretched. In the test, the yield strength and ultimate strength were measured, and the test results are shown in [Tab. 3](#).

**Table 1:** Test mix ratio (kg/m<sup>3</sup>)

Recycled coarse aggregate substitution rate	Cement	Fly ash	Silica Fume	Water	sand	Stone	Recycled coarse aggregate	Water reducing agent	Steel fiber
0	432	54	54	194.4	699.55	966.05	0	10.8	79
50%	432	54	54	194.4	699.55	483.02	483.02	10.8	79
100%	432	54	54	194.4	699.55	0	966.005	10.8	79

**Table 2:** Concrete mechanical performance indicators

Recycled coarse aggregate substitution rate	Cube compressive strength/MPa	Vertical tensile strength/MPa	Elastic Modulus/MPa
0	50.60	2.14	$3.47 \times 10^4$
50%	51.35	1.40	$3.48 \times 10^4$
100%	52.03	2.09	$3.49 \times 10^4$

**Table 3:** Mechanical performance indexes of steel bars

Species	Rebar grade	Diameter/mm	Yield Strength/MPa	Ultimate strength/MPa	Elongation after breaking/%
Longitudinal rib	HRB400	16	498	613	26
Stirrup	HRB400	8	437	653	13

Note: HRB represents the hot rolled ribbon bar.

A total of four specimens were designed for the experiment, and the specimen size was 250 mm × 250 mm × 500 mm. The shear span ratio of the column is 2; the replacement rates of recycled coarse aggregate are 0, 50% and 100%; and the volume of steel fiber is 1.0%. There are eight longitudinal bars in total, equipped with HRB400 steel bars with a diameter of 16 mm, and they are evenly distributed along the section. The reinforcement ratio is 2.57%. The stirrup configuration is HRB400 steel bars with a diameter of 8 mm and a spacing of 100 mm, the ratio of stirrups is 1.37%, and the thickness of the concrete clear cover is 15 mm. Strain gauges are arranged symmetrically in the middle of the corner steel bars, and the layout points of the steel bars of the specimen are shown in Fig. 1. A 10 mm-thick Q235 steel plate is added to the upper and lower ends of the column to avoid local pressure damage to the column. When the specimen reaches 50% of the ultimate carrying capacity, CFRP sheet is attached for reinforcement. When the specimen is loaded to 50% of the ultimate load, internal micro-cracks are generated and are in a stable development state. At this time, CFRP cloth can effectively play the role of reinforcement to strengthen the carrying capacity of the specimen. After pre-damage, no obvious cracks are produced on the surface of the specimen. The pre-damaged specimen is reinforced and pasted with two layers of CFRP cloth. The pasting area is 1,200 mm long and 500 mm wide. The detailed parameters of each group of specimens are shown in Tab. 4.

An electro-hydraulic servo universal testing machine (10000 kN) was used for the loading of this experiment, which is shown in Fig. 2. The force-controlled loading method was adopted in the whole process of the uniform axial compression of the specimens. Two displacement meters are attached to the lower pressure plate of the testing machine, and the accuracy of the displacement meters is 0.01 mm. Preloading is conducted before the formal test to ensure that the measuring instruments are in normal working condition. The loading rate of the column is 1.5 kN/s. In the loading method used herein, load increment before cracking of the column is 100 kN, and the load increment after the cracking is 200 kN. After each level of loading is completed, it is kept stable for 3 minutes, and the displacement meter data is collected. The load value is measured by the device's own force sensing system. The loading system is shown in the Fig. 3.

### 3 Test Results and Analysis

#### 3.1 Destruction Form

When the monotonically loaded specimen SC-1 was loaded to 1200 kN, cracks appeared at the lower corners of the specimen. When loaded to 1300 kN, vertical cracks appeared in the middle of the specimen. With the increase in the load, the number of cracks increased, and the length of the cracks

gradually increased. The width of the cracks increased from the ends to the middle of the specimen. When loaded to 1900 kN, the specimen made noise, cracks developed and widened rapidly, and the maximum crack width was 1 mm. When the loading was continued, the number of cracks on the concrete surface no longer increased. The original crack width continued to develop, and the concrete in the middle of the specimen bulged along the cracks and separated from the internal steel bars. When the load was 3100 kN, the specimen experienced axial compression failure, and the final failure diagram is shown in Fig. 4a.

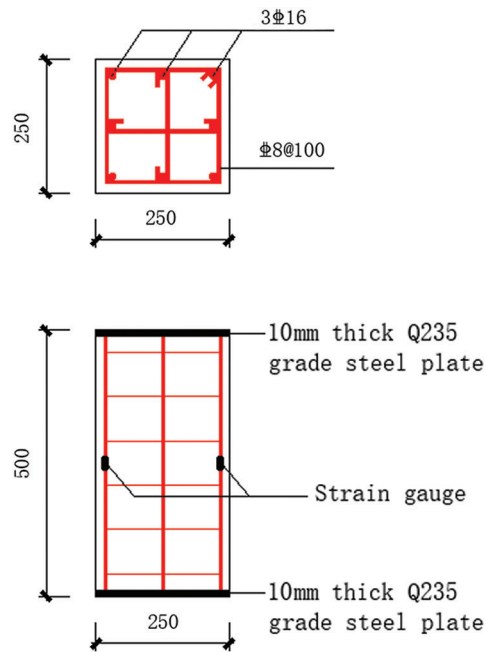


**Figure 1:** Reinforcement form and cross-sectional schematic diagram of components

**Table 4:** Component design parameters

Component number	Column section size/mm <sup>2</sup>	Recycled coarse aggregate substitution rate	Restraint	Loading method
SC-1	250 × 250	0	no	Monotonic loading
SC-2	250 × 250	50%	no	Monotonic loading
SC-3	250 × 250	100%	no	Monotonic loading
SC-4	250 × 250	100%	CFRP	Monotonic loading

The destruction process of specimens SC-2 and SC-3 was similar to that of specimen SC-1. The specimen SC-2 cracked at 1100 kN. When loaded to 1800 kN, the maximum crack width was about 1 mm. When the load was 2500 kN, the specimen was damaged, and the final damage diagram is shown in Fig. 4b. The first crack appeared when the specimen SC-3 was loaded to 1300 kN. When loaded to 2100 kN, the maximum crack width was 1mm. When the load was 3200 kN, axial compression failure occurred, and the final failure diagram is shown in Fig. 4c. During the loading process of specimen SC-4, there was no crack on the surface. When loaded to 3350 kN, the carbon fiber cloth cracked and produced noise. When loading was continued up to 3740 kN, the carbon fiber cloth was separated from the concrete surface, the internal cracks of the specimen developed fully, and the axial compression failure characteristics were obvious. The final destruction diagram is shown in Fig. 4d.

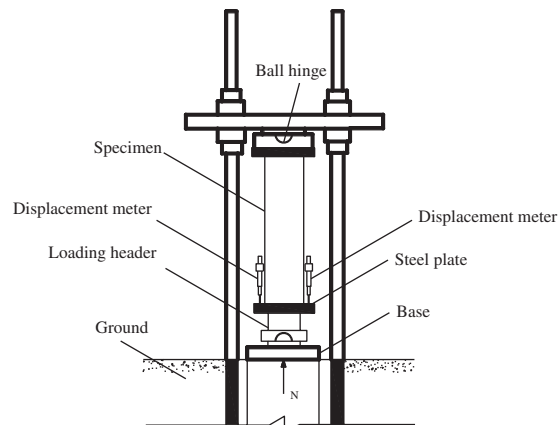


**Figure 2:** Monotonic loading device

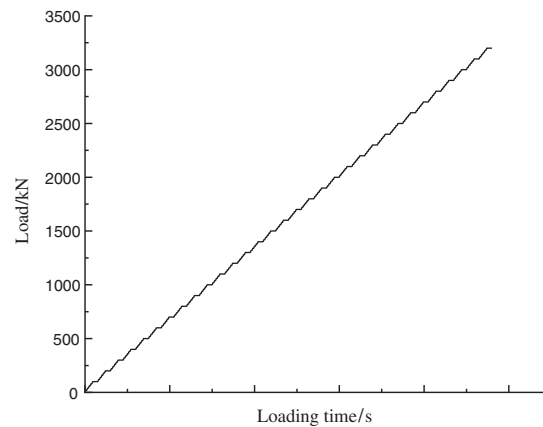


**Figure 3:** The diagram of load system

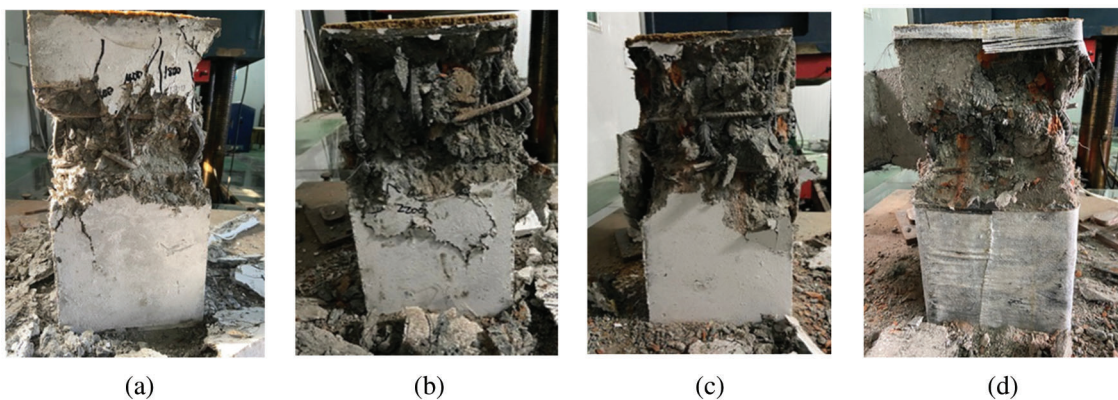


**Figure 4:** Destruction diagram of each component (a) SC-1 (b) SC-2 (c) SC-3 (d) SC-4

### 3.2 Load-Vertical Displacement Curve

Fig. 5 shows the load-vertical displacement curves of specimens SC-1~SC-3 under different replacement rates of recycled coarse aggregate. It can be seen from the figure that when the replacement rate of recycled aggregate was 100%, the curve showed an obvious yield platform, indicating that the specimen had better ductility. This is mainly because the specimen used large-size recycled aggregate to

form a skeleton in the concrete which played a supporting role. Compared with specimen SC-1, the ultimate carrying capacity of specimen SC-3 increased by 5%, and the ultimate carrying capacity of specimen SC-2 reduced by 6%, indicating that the coarse aggregate of recycled aggregate concrete had less influence on the carrying capacity of the column. Compared with specimen SC-2, specimen SC-3 displayed higher rigidity. This is mainly due to the fact that the replacement rate of large-size recycled aggregate was 100% in recycled aggregate concrete, and the internal recycled aggregate formed a relatively strong skeleton. Therefore, its rigidity was relatively high. The vertical displacements corresponding to the ultimate load points of SC-2 and SC-3 were close. Compared with natural concrete, the specimens showed good deformation performance before reaching the ultimate state of carrying capacity. After the peak point of natural concrete, the curve dropped steeply and the ductility was poor.

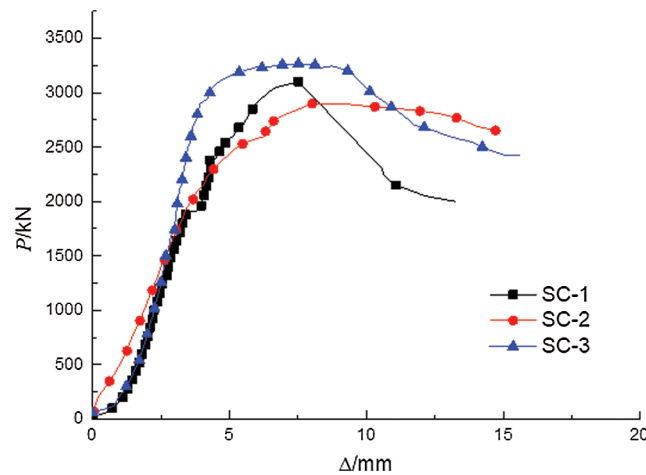


**Figure 5:** Load-vertical displacement curves of components under different regeneration substitution rates

Fig. 6 presents the load-vertical displacement curve diagram of the specimen without and with pre-damage reinforcement at 100% replacement rate of recycled coarse aggregate. At the beginning of loading, the structural rigidity of the pre-damaged reinforced specimen was similar to that of the unreinforced specimen. Wrapping with CFRP sheet compensated for the damage caused by the pre-damage. As the load continued to increase, CFRP sheet began to exert its restraining effect, the stiffness of the specimen gradually increased, and the ability to resist deformation was enhanced. Compared with the unreinforced specimen, the ultimate carrying capacity of the pre-damaged reinforced specimen increased by about 14.5%, and the peak vertical displacement reduced by 17.1%. These results indicate that pasting CFRP sheet can improve the axial load carrying capacity of the specimen and the ability to resist deformation.

### 3.3 Vertical Load-Rebar Strain Curve

Fig. 7 shows the steel bar load-strain curve of each specimen, where strain gauges A and B are the longitudinal reinforcement strain gauges on one side of the specimen. It can be seen from the figure that the longitudinal bars of each specimen exhibited the yield strain of  $2490 \mu\epsilon$ . From the load-strain curves of SC-1~SC-3 steel bars, it can be seen that before the specimen reached the ultimate load, the strain value of each longitudinal steel bar was small, and the load was mainly borne by the concrete. After the specimen reached the ultimate load, the concrete was crushed and the steel bar yielded. Compared with the specimens SC-1~SC-3, the lower slope of the load-strain curve of the SC-4 steel bar in the early stage was mainly due to the failure of the specimen during the pre-damage, the deterioration of the rigidity, the internal cracks, and the increase in the degree of participation of the steel bar. As the load increased, CFRP sheet began to exert its restraint effect. Consequently, the structural rigidity of the specimen gradually increased, and the overall resistance to deformation was enhanced.

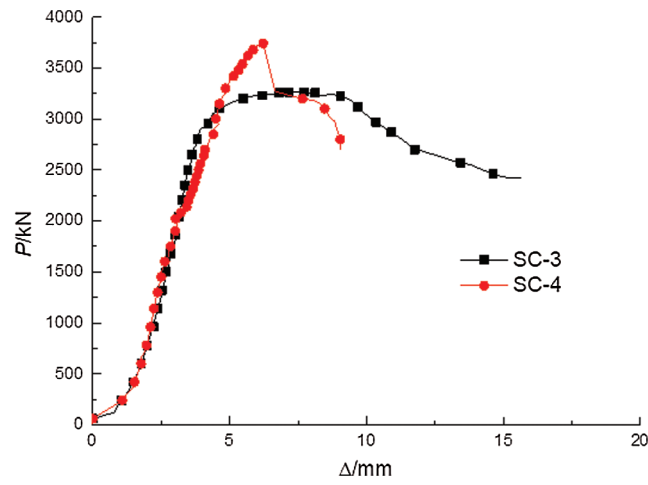


**Figure 6:** Load-vertical displacement curve of member SC-3 and SC-4

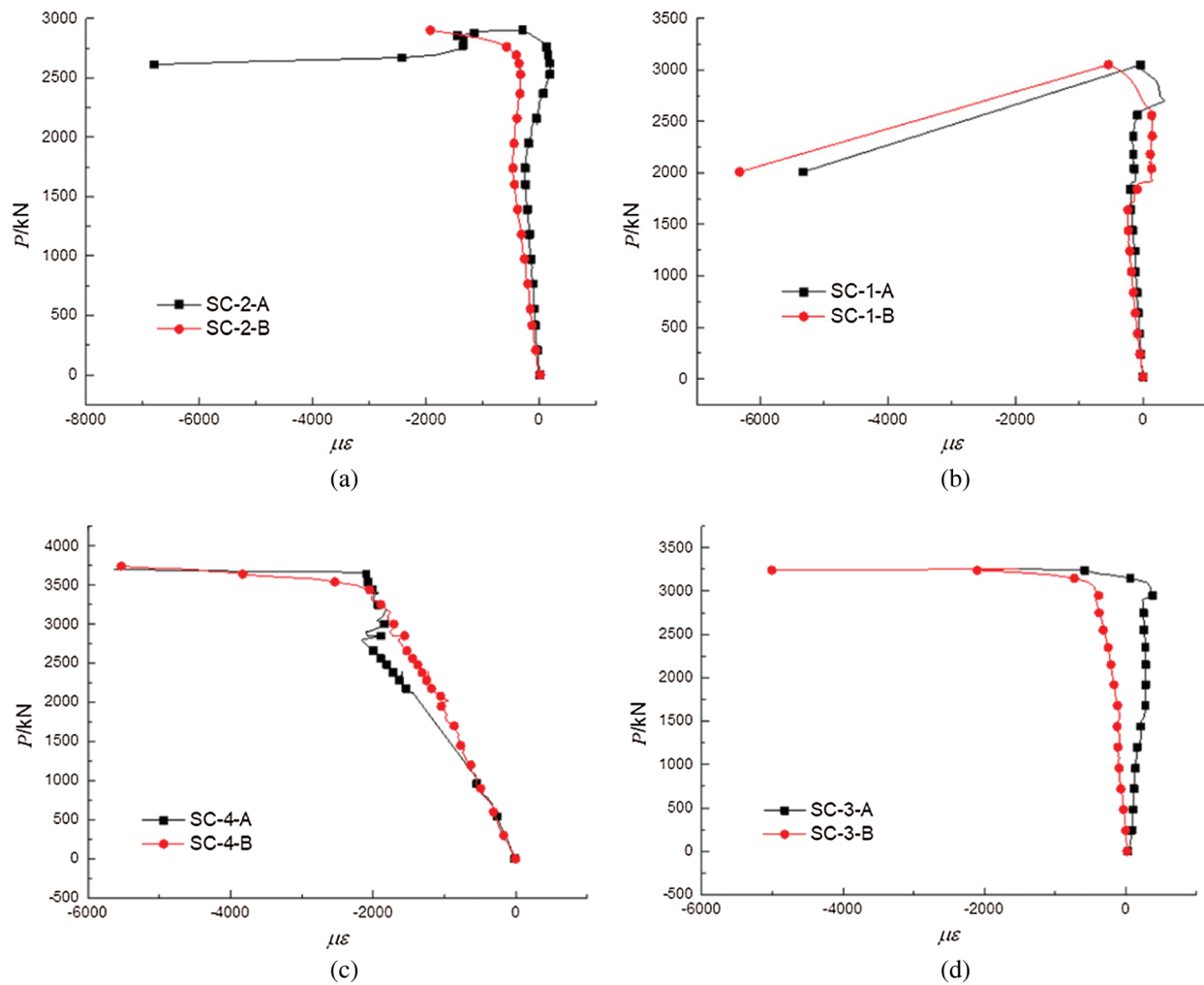


**Figure 7:** Vertical load-rebar strain curve of specimens (a) SC-1 (b) SC-2 (c) SC-3 (d) SC-4

#### 4 Numerical Simulation Analysis

On the basis of the experiment, the ABAQUS finite element software was used for parameter analysis. In this paper, the concrete and steel plate adopted eight-node three-dimensional integral solid element (C3D8R), the reinforcement adopted three-dimensional truss element (T3D2), and the carbon fiber cloth adopted three-dimensional membrane element (M3D4R). The finite element model was implemented according to the separation method. The constitutive model of concrete used the damage plasticity model in ABAQUS. In the simulation, it was assumed that no bond slip occurred between the steel bar and the concrete. The built-in area constraint was adopted between the steel bar and the concrete, and the binding constraint was adopted between the carbon fiber cloth and the concrete. The reference point was coupled with the surface of the loading head. The loading head and the column end created frictional contact. The normal behavior in the contact was selected as “hard” contact, and the constraint execution method was penalty. When the grid was divided, the size of the concrete structural unit was a cube unit with a side length of 15 mm. The CFRP cloth used a 45 mm side membrane unit, and the upper and lower steel plates used a 20 mm side cube unit. The longitudinal ribs and stirrups used truss elements with a side length of 16 mm.

For natural concrete under compression, the uniaxial compression stress-strain constitutive relationship of concrete is recommended in the concrete structure design code. The compression stress-strain curve of recycled aggregate concrete is obtained from a literature formula [21]. In the simulation, the cubic compressive strength of concrete adopted the actual measured value. The elastic modulus of recycled aggregate concrete was calculated by the calculation formula proposed in literature [22], and the Poisson’s ratio was 0.2. The reinforcement adopted the isotropic elastic-plastic model provided in the ABAQUS software, and the stress-strain relationship adopted the “elastic-strengthening” double-broken line model. The elastic modulus of the strengthened section was 0.01 times the initial elastic modulus. In the simulation, the yield strength and elastic modulus of the steel bars were measured by actual values, and the Poisson’s ratio was 0.3. The damage and reinforcement of the specimens used the “life and death element method” for modeling and analysis. The displacement control loading method was adopted in the whole process of the simulation of the axial compression of each specimen.

The formula for calculating the elastic modulus of recycled aggregate concrete is as follows (with Poisson’s ratio of 0.2):

$$E_{c,r} = (1 - 0.30\delta) \frac{10^5}{2.2 + \frac{34.7(1 - 0.15\delta)}{f_{cu,r}}} \quad (1)$$

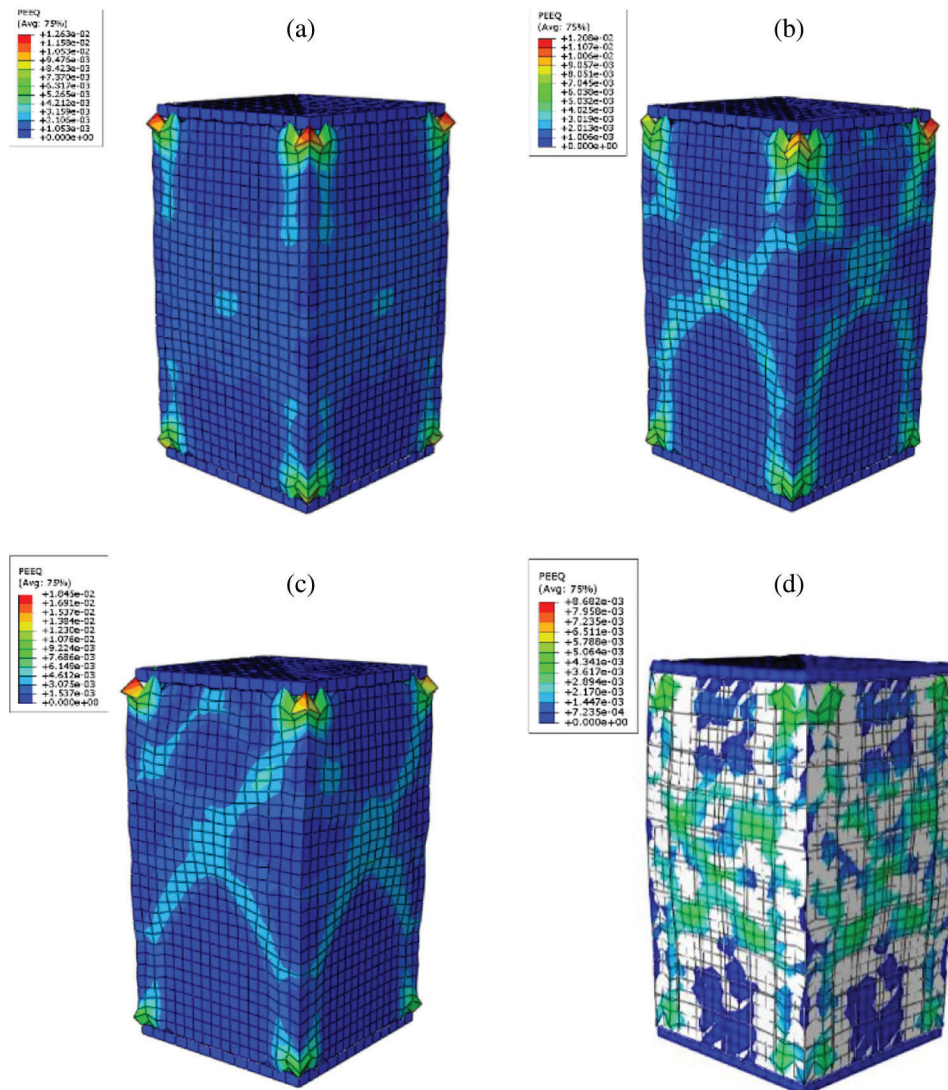
where,  $f_{cu,r}$  is the compressive strength of recycled aggregate concrete cube; and  $\delta$  is the replacement rate of recycled aggregate.

Sidoroff proposed the calculation formula of concrete damage factor based on the principle of energy equivalence as follows:

$$d = 1 - \sqrt{\frac{\sigma}{(E_0 \varepsilon)}} \quad (2)$$

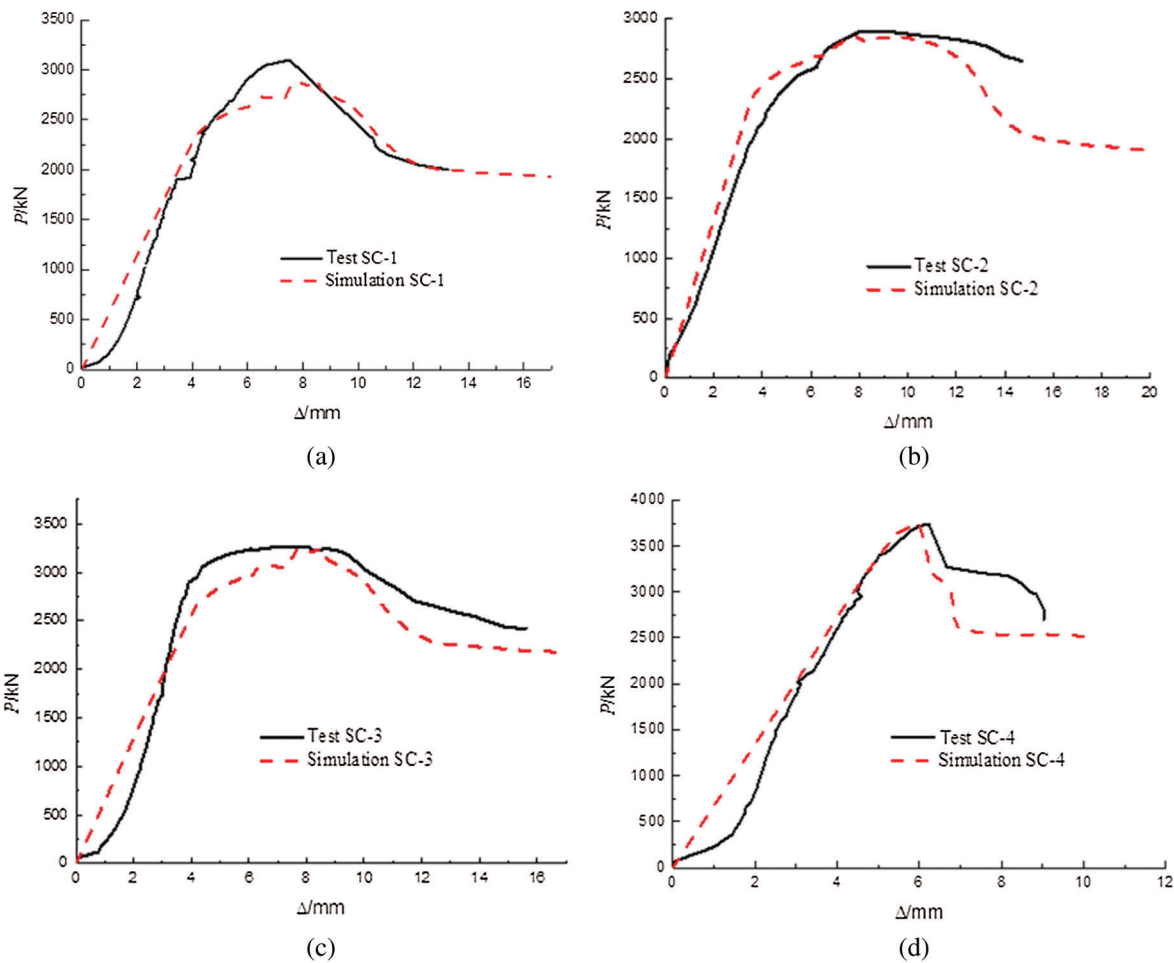
where,  $d$  is the plastic damage factor of concrete;  $\sigma$  is the concrete stress;  $\varepsilon$  is the concrete strain; and  $E_0$  is the initial elastic modulus of concrete.

Fig. 8 presents a concrete equivalent plastic strain diagram of the calculation results of the finite element analysis model of each specimen. It can be seen from the figure that the stress in the middle area of the test piece was relatively large, and the steel bar bulged outwards, showing the characteristics of axial compression failure, which is more consistent with the final failure mode of each test.



**Figure 8:** Concrete equivalent plastic strain diagram of each specimen (a) SC-1 (b) SC-2 (c) SC-3 (d) SC-4

Fig. 9 presents the comparison of simulated and experimental load-vertical displacement curves. The simulated curve and the experimental curve were in good agreement. At the initial stage of specimen loading, the ascending section of the load-displacement curve of each specimen was basically linear. As the load increased, the specimen entered the yield stage, and continued to load. After reaching the peak load, the load dropped rapidly and the specimen was destroyed. The results show that the error between the simulated value and the test value of the specimen peak load was within 7%, and the vertical displacement error corresponding to the peak load did not exceed 8%. The ABAQUS simulation results were generally in good agreement with the test results. Tab. 5 shows the comparison between the simulation and the test results, which indicates that the finite element analysis method can simulate the axial compression performance of the specimen accurately.



**Figure 9:** Comparison of simulated load-vertical displacement curves of component test (a) SC-1 (b) SC-2 (c) SC-3 (d) SC-4

**Table 5:** Comparison of simulated and experimental values

Component	Simulation value/kN	Test value/kN	Relative error/%
SC-1	2852.81	3100	7.97
SC-2	2815.23	2900	2.92
SC-3	3234.82	3265	0.92
SC-4	3717.99	3740	0.59

### 5 Compressive Carrying Capacity Calculation

With reference to the calculation formula for the axial compression carrying capacity of natural reinforced concrete columns proposed in the current code “Specification for Concrete Structure Design” GB 50010-2010, combined with the characteristics of recycled aggregate concrete and related test data, the steel fiber under different replacement rates of recycled coarse aggregate was analyzed. In this paper, the stress state when each member reached the peak load was selected as the reference state for the

calculation of compressive carrying capacity. Then, the calculation formula for the axial compression carrying capacity of aggregate recycled aggregate concrete columns was proposed.

The formula for calculating the compressive carrying capacity of natural reinforced columns under load proposed in the code is as follows:

$$N_u = 0.9\varphi(f_c A + f_y A_s) \quad (3)$$

In the formula,  $N_u$  is the design value of axial force,  $f_c$  is the design value of concrete axial compressive strength,  $f_y$  is the yield strength of the compressive strength,  $A_s$  is the area of the compressed steel bar,  $A$  is the cross-sectional area of the column, and  $\varphi$  is the stability coefficient of the column under compression (for short column  $\varphi = 1.0$ ).

Based on the comparison between the calculated value of the current code and the test value of the specimen, the method of introducing the concrete strength reduction coefficient to calculate the axial compression carrying capacity of the specimen was proposed. The calculation formula for the axial compression carrying capacity of recycled aggregate concrete columns is as follows:

$$N_u = 0.9\varphi(\alpha f_c A + f_y A_s) \quad (4)$$

In the formula,  $\alpha$  is the compression strength reduction coefficient of recycled aggregate concrete. According to the test results,  $\alpha = (1 - 1.0r)$  is proposed. When the specimen is a normal concrete column,  $\alpha$  is taken as 1.0 in the formula.

The experimental values of recycled aggregate concrete columns under different replacement rates were substituted into the formula, and the calculated values were compared with the experimental values. The comparison results are shown in Tab. 6. It can be seen that the calculated results of the formula were similar to the test results, and the error was relatively small. Therefore, this formula is suitable for calculating the axial compression carrying capacity of steel fiber aggregate recycled aggregate concrete short columns.

**Table 6:** Comparison of calculated and experimental values

Component	Calculated/kN	Test value/kN	Relative error/%
SC-1	3262.63	3100	5.25
SC-2	3149.03	2900	8.59
SC-3	3026.82	3265	7.29

## 6 Conclusion

In this paper, axial compression performance tests were performed on recycled aggregate concrete columns. The main conclusions are as follows:

- (1) The use of recycled coarse aggregate improved the ductility of recycled aggregate concrete columns, and the deformation performance of the specimens was better. At all recycled aggregate replacement levels, the performance of recycled aggregate short columns are similar to that of natural aggregate concrete short columns;
- (2) The use of CFRP sheet to reinforce the specimen can compensate for the damage caused by the pre-damage to the specimen. As the load increased, the CFRP sheet exerted its restraining effect. The

stiffness of the specimen gradually increased, the resistance to deformation was enhanced, and the carrying capacity of the column was improved.

- (3) The ABAQUS finite element analysis based on the parameters of the recycled aggregate concrete column obtained from the experiment can better reflect the characteristics of the axial compression force and deformation of the recycled aggregate concrete column. The simulated column deformation behavior was in good agreement with the experimental result. The simulated load-displacement curve was also consistent with the experimental data.
- (4) Based on the specification, the results of the calculation method for the axial compression carrying capacity of recycled aggregate concrete columns were in good agreement with the test results. Therefore, the proposed method is suitable for the calculation of the axial compression carrying capacity of recycled aggregate concrete columns under different parameters.

**Funding Statement:** The authors received no specific funding for this study.

**Conflicts of Interest:** The authors declare that they have no conflicts of interest to report regarding the present study.

## References

1. Vivian, W. Y., Tam, M. S., Ana, C. J. E. (2018). A review of recycled aggregate in concrete applications (2000–2017). *Construction and Building Materials*, 172, 272–292.
2. Thomas, C., Setién, J., Polanco, J. A., Alaejos, P., de Juan, M. S. (2013). Durability of recycled aggregate concrete. *Construction and Building Materials*, 40, 1054–1065.
3. Kou, S. C., Poon, C. S. (2013). Long-term mechanical and durability properties of recycled aggregate concrete prepared with the incorporation of fly ash. *Cement and Concrete Composites*, 37, 12–19.
4. Dimitriou, G., Savva, P., Petrou, M. F. (2018). Enhancing mechanical and durability properties of recycled aggregate concrete. *Construction and Building Materials*, 158, 228–235.
5. Carneiro, J. A., Lima, P., Leite, M. B., Filho, R. T. (2014). Compressive stress-strain behavior of steel fiber reinforced-recycled aggregate concrete. *Cement & Concrete Composites*, 46, 65–72.
6. Ramesh, R. B., Mirza, O., Kang, W. H. (2019). Mechanical properties of steel fiber reinforced recycled aggregate concrete. *Structural Concrete*, 20(2), 745–755.
7. Xiao, J. Z., Li, J. B., Sun, Z. P. (2004). Study on compressive strength of recycled aggregate concrete. *Journal of Tongji University (Natural Science)*, 32(12), 1558–1561.
8. Etxeberria, M., Vázquez, E., Marí, A., Barra, M. (2007). Influence of amount of recycled coarse aggregates and production process on properties of recycled aggregate concrete. *Cement and Concrete Research*, 37(5), 735–742.
9. Liu, C., Wu, Y., Gao, Y., Tang, Z. (2021). Experimental and numerical analysis of high-strength concrete beams including steel fibers and large-particle recycled coarse aggregates. *Fluid Dynamics & Materials Processing*, 17(5), 947–958. DOI 10.32604/fdmp.2021.016283.
10. Cao, W. L., Li, D. H., Zhou, Z. Y. (2013). Experimental study on axial compression performance of full scale recycled concrete columns. *Structural Engineers*, 29(6), 144–150.
11. Cao, W., Cao, H., Qiao, Q., Zhang, J., Shen, H. (2016). Experimental study on compression performance of high strength full scale recycled rc columns under small eccentric loading. *Journal of Building Structures*, 37, 43–50.
12. Cao, W., Cao, H., Jiang, W., Chen, C., Shen, H. (2016). Calculation analysis of eccentric compression performance of full scale recycled rc columns. *Journal of Natural Disasters*, 25(3), 130–136.
13. Choi, W. C., Yun, H. D. (2012). Compressive behavior of reinforced concrete columns with recycled aggregate under uniaxial loading. *Engineering Structures*, 41, 285–293.
14. Xu, J. J., Chen, Z. P., Xiao, Y., Demartino, C., Wang, J. H. (2017). Recycled aggregate concrete in frp-confined columns: A review of experimental results. *Composite Structures*, 174, 277–291.
15. Xiong, M. X., Xu, Z., Chen, G. M., Lan, Z. H. (2020). FRP-confined steel-reinforced recycled aggregate concrete columns: Concept and behaviour under axial compression. *Composite Structures*, 246, 112408.

16. Sunayana, S., Barai, S. V. (2019). Performance of fly ash incorporated recycled aggregates concrete column under axial compression: Experimental and numerical study. *Engineering Structures*, 196, 109258.
17. Wu, B., Liu, L., Zhao, X. L. (2016). Test study on uniaxial compressive behaviors of compound concrete made of normal-strength demolished concrete lumps and high-strength self-compacting concrete. *Journal of Building Structures*, 37(S2), 73–78.
18. Wu, B., Liu, W., Liu, Q. X., Xu, Z. (2010). Test on axial behavior of reinforced concrete columns filled with demolished concrete segment/lump. *Seismic Engineering and Reinforcement*, 32(3), 81–85+98.
19. Jia, M. L. (2020). *Research on axial compression performance of recycled concrete columns constrained by CFRP (Master's Thesis)*. Xi'an University of Technology.
20. Huang, C. (2020). *Study on the axial stress behavior of recycled concrete columns constrained by CFRP (Master's Thesis)*. Xi'an University of Technology.
21. Xiao, J. Z. (2007). Experimental investigation on complete stress-strain curve of recycled concrete under uniaxial loading. *Journal of Tongji University (Natural Science)*, 35(11), 1445–1449.
22. Zhou, L., Yang, Z., Wu, X. P. (2017). Calculation equation study and calculation error analysis of elastic modulus on recycled aggregate concrete. *Concrete*, (5), 143–148.